

# Variational formulation of the Generalized Navier Boundary Condition.

J.-F. Gerbeau<sup>1</sup> and T. Lelièvre<sup>2</sup>

<sup>1</sup> INRIA, Rocquencourt, B.P.105,  
78153 Le Chesnay Cedex, France  
jean-frederic.gerbeau@inria.fr

<sup>2</sup> CERMICS, Ecole Nationale des Ponts et Chaussées,  
6 & 8 Av. Pascal, 77455 Champs-sur-Marne, France  
lelievre@cermics.enpc.fr

8th June 2006

## Abstract

In this paper, we propose an Arbitrary Lagrangian Eulerian (ALE) formulation of the Generalized Navier Boundary Condition introduced in [14, 15] to model the displacement of the contact line of an interface in two-fluid flows. Owing to these boundary conditions, it is possible to circumvent the incompatibility between the classical no-slip boundary condition and the fact that the contact line of the interface on the wall is actually moving. We present some results on the stability of the numerical scheme in energy norm. We show the validity of the approach by numerical experiments on two-fluid flows in narrow channels.

**Keywords:** Generalized Navier Boundary condition, surface tension, Arbitrary Lagrangian Eulerian formulation, two-fluid flows, geometric conservation law, energy estimates.

## 1 Introduction

A difficult problem in the modelling of two-fluid flows in a bounded domain concerns the displacement of the contact line, namely the points which are at the intersection of the boundary of the domain and the interface separating the two fluids. The difficulty comes from the fact that:

- the interface follows the fluid motion: the normal velocity of a point on the interface is the normal velocity of the fluid particle at the same point,
- the fluid particles near the boundary of the domain tend to have the same velocity as the points of the boundary.

Thus, if the velocity of the points on the boundary of the domain is zero (classical no-slip condition for a viscous fluid on a fixed wall), the moving contact line does not move: this is the so-called moving contact line problem. This is actually a modelling problem: an appropriate boundary conditions regarding the fluid particles on the moving contact line is required. We refer to the review paper [15] for an introduction to the moving contact line problem.

An appropriate boundary condition to tackle this problem which has recently been proposed in [14] is the Generalized Navier Boundary Condition (GNBC). Starting from the classical Navier boundary condition (which relates the slip velocity relative to the moving wall to the tangential stress exerted by the wall), the authors introduce an additional term located on the moving contact line, which enables a pure slip on this line. The GNBC is found to be in very good agreement with detailed molecular dynamics simulations (see [14, 15]).

In this paper, we show that the GNBC can be very naturally implemented in an Arbitrary Lagrangian Eulerian (ALE) formulation. In [14, 15], this boundary condition is used in a phase-field formulation to take into account the displacement of the interface between the two fluids. We believe it is interesting to discuss its implementation in an ALE setting since it leads to a very natural variational formulation, with fewer numerical parameters than in a phase-field formulation (for which a free energy for the order parameter needs to be introduced, for example). The main drawback of the ALE method compared to other methods to follow a moving interface (like volume of fluid method [12, 11]), level sets method [18, 16] or phase-field formulation) is that it does not allow large motion of the interface, leading for example to a change of topology of the domains occupied by each fluid. On the other hand, it is generally admitted that it is the method of choice when a precise modelling of the position of the interface is required. They are thus many applications where the ALE method can be used (see [7] or Chapter 6 in [8] for application to the modelling of aluminium electrolysis cells, and Section 5 for an application to flows in narrow channels).

In Section 2, the GNBC is introduced. The ALE formulation used to implement this boundary condition is presented in Section 3. We then present some results on the energy conservation properties of the numerical scheme in Section 4. Finally, Section 5 is devoted to some numerical experiments.

## 2 The Generalized Navier Boundary Condition

We are interested in the two-fluid Navier-Stokes equations, posed on a bounded smooth domain  $\Omega \subset \mathbb{R}^d$  (with  $d = 2$  or  $d = 3$ ), and the time interval  $(0, T)$ :

$$\begin{cases} \frac{\partial(\rho \mathbf{u})}{\partial t} + \operatorname{div}(\rho \mathbf{u} \otimes \mathbf{u}) - \operatorname{div}(\eta(\nabla \mathbf{u} + \nabla \mathbf{u}^T)) = -\nabla p + \gamma H \mathbf{n}_\Sigma \delta_\Sigma + \mathbf{f}, \\ \operatorname{div}(\mathbf{u}) = 0, \\ \frac{\partial \rho}{\partial t} + \operatorname{div}(\rho \mathbf{u}) = 0. \end{cases} \quad (1)$$

The equation is posed in the distributional sense. The velocity is denoted by  $\mathbf{u}$ , the density by  $\rho$ , the viscosity by  $\eta$  and the pressure by  $p$ . The vector  $\mathbf{f}$  denotes an external force (like the gravity force for example), and the term  $\gamma H \mathbf{n}_\Sigma \delta_\Sigma$  is the surface tension term that we will describe in detail below. The system is complemented by initial conditions ( $\mathbf{u}(t = 0), \rho(t = 0)$ ). We suppose that  $\rho(t = 0)$  takes two different values  $\rho_1$  and  $\rho_2$ . This property is then conserved as time evolves for the function  $\rho$  so that each fluid is distinguished from the other by its density. In the following we denote by

$$\Omega_i(t) = \left\{ \mathbf{x} \in \mathbb{R}^d, \rho(t, \mathbf{x}) = \rho_i \right\} \quad (2)$$

the domain occupied at time  $t$  by the fluid  $i$ . We suppose that  $\Omega_i(t)$  is a smooth domain, and we denote by

$$\Sigma(t) = \partial\Omega_1(t) \cap \partial\Omega_2(t) \quad (3)$$

the interface between the two liquids. The viscosity  $\eta$  may depend on the fluid, so that  $\eta = \eta(\rho)$  in (1). We denote in the following by

$$\boldsymbol{\sigma} = \eta (\nabla \mathbf{u} + \nabla \mathbf{u}^T) \quad (4)$$

the viscous stress tensor. In the surface tension term  $\gamma H \mathbf{n}_\Sigma \delta_\Sigma$ ,  $\gamma$  is the surface tension coefficient between the two fluids (which we suppose to be constant in the following),  $\mathbf{n}_\Sigma$  is the unit outward vector normal to  $\Omega_1$  (see Figure 1) and  $H$  is the mean curvature of the interface  $\Sigma$  positively counted with respect to the normal  $\mathbf{n}_\Sigma$ . The distribution  $\delta_\Sigma$  is defined by: for any smooth function  $\psi$

$$\langle \delta_\Sigma, \psi \rangle = \int_\Sigma \psi d\sigma_\Sigma \quad (5)$$

where  $\sigma_\Sigma$  denotes the Lebesgue measure (*i.e.* the surface measure) on  $\Sigma$ .

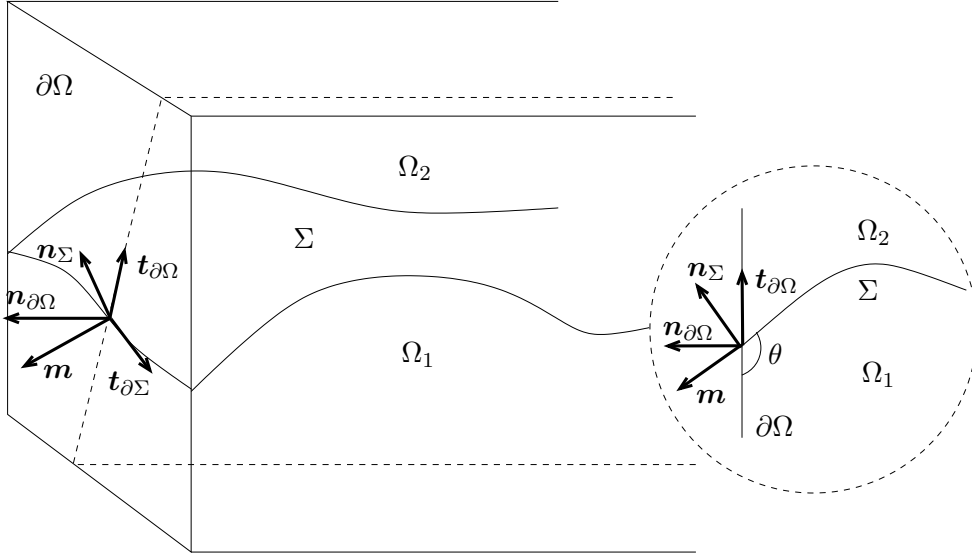


Figure 1: The domain  $\Omega$  and various unit vectors. The 2d picture (in the dotted line circle) represents the vectors in the plane orthogonal to  $\mathbf{t}_{\partial\Sigma}$ .

Let us now describe the boundary conditions. We suppose first the non-penetrability condition:

$$\mathbf{u} \cdot \mathbf{n}_{\partial\Omega} = 0 \text{ on } \partial\Omega, \quad (6)$$

where  $\mathbf{n}_{\partial\Omega}$  denotes the unit outward vector normal to  $\Omega$  (see Figure 1). In order the problem to be well posed, we then need to prescribe a boundary condition on the tangential components of the stress  $\boldsymbol{\sigma} \mathbf{n}_{\partial\Omega}$  or on the tangential components of the velocity. Let us introduce (see Figure 1) the following vectors defined on the boundary  $\partial\Sigma$  of the interface:  $\mathbf{t}_{\partial\Sigma} = \mathbf{n}_\Sigma \times \mathbf{n}_{\partial\Omega}$  the tangent vector to  $\partial\Sigma$ ,  $\mathbf{m} = \mathbf{t}_{\partial\Sigma} \times \mathbf{n}_\Sigma$  and  $\mathbf{t}_{\partial\Omega} = \mathbf{n}_{\partial\Omega} \times \mathbf{t}_{\partial\Sigma}$ . Both sets of vectors  $(\mathbf{t}_{\partial\Sigma}, \mathbf{n}_\Sigma, \mathbf{m})$  and  $(\mathbf{t}_{\partial\Sigma}, \mathbf{t}_{\partial\Omega}, \mathbf{n}_{\partial\Omega})$  are positively oriented orthonormal basis.

The GNBC writes (see [15]): for any vector  $\boldsymbol{\tau}$  tangent to  $\partial\Omega$ ,

$$\beta (\mathbf{u} - \mathbf{u}^b) \cdot \boldsymbol{\tau} + \boldsymbol{\sigma} \mathbf{n}_{\partial\Omega} \cdot \boldsymbol{\tau} + \gamma (\mathbf{m} \cdot \mathbf{t}_{\partial\Omega} - \cos(\theta_s)) \mathbf{t}_{\partial\Omega} \cdot \boldsymbol{\tau} \delta_\Sigma = 0, \quad (7)$$

where  $\mathbf{u}^b$  is the velocity of the boundary, so that  $\mathbf{u} - \mathbf{u}^b$  is the slip velocity (which is tangent to  $\partial\Omega$ ),  $\beta$  is the slip coefficient,  $\gamma$  is again the surface tension coefficient between

the two fluids and  $\theta_s$  is the static contact angle at the solid surface. The distribution  $\delta_{\partial\Sigma}$  is defined accordingly with (5) by: for any smooth function  $\psi$

$$\langle \delta_{\partial\Sigma}, \psi \rangle = \int_{\partial\Sigma} \psi dl_{\partial\Sigma} \quad (8)$$

where  $l_{\partial\Sigma}$  denotes the Lebesgue measure (*i.e.* the length measure) on the curve  $\partial\Sigma$ .

Notice that the term  $(\mathbf{m} \cdot \mathbf{t}_{\partial\Omega} - \cos(\theta_s))$  measures the difference between the dynamic contact angle  $\theta$  between the interface  $\Sigma$  and the boundary  $\partial\Omega$  (we choose the convention that this angle is measured in the fluid 1, see Figure 1) and the static contact angle  $\theta_s$ , which is part of the data.

The usual Navier boundary condition is  $\beta(\mathbf{u} - \mathbf{u}^b) \cdot \boldsymbol{\tau} + \sigma \mathbf{n}_{\partial\Omega} \cdot \boldsymbol{\tau} = 0$ . The additional term (the so-called uncompensated Young stress, see [15])  $\gamma(\mathbf{m} \cdot \mathbf{t}_{\partial\Omega} - \cos(\theta_s)) \mathbf{t}_{\partial\Omega} \cdot \boldsymbol{\tau} \delta_{\partial\Sigma}$  is concentrated along the boundary of the interface.

### 3 Variational formulation and discretization

The aim of this section is to derive a variational formulation of the system of equations (1), together with the boundary conditions (6)–(7).

#### 3.1 The weak ALE formulation

We refer to [6] or to Chapter 5 in [8] for more details about the ALE formulation. We assume that for any time  $t \geq 0$ , there exists a smooth and bijective mapping  $\hat{\mathcal{A}}_t$  from a reference domain  $\hat{\Omega}$  (divided into two separate subdomains  $\hat{\Omega}_1$  and  $\hat{\Omega}_2$  such that  $\overline{\hat{\Omega}} = \overline{\hat{\Omega}_1} \cup \overline{\hat{\Omega}_2}$ ) to the current domain  $\Omega$  such that  $\hat{\mathcal{A}}_t(\hat{\Omega}_i) = \Omega_i(t)$  (see Figure 2). The inverse function (with respect to the space variable) of  $\hat{\mathcal{A}}_t$  is denoted  $\hat{\mathcal{A}}_t^{-1}$ .

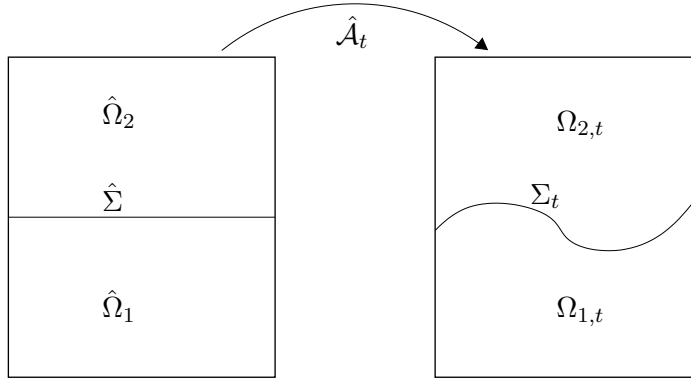


Figure 2: The partition of the domain  $\Omega$ .

The velocity of the domain  $\hat{\mathbf{w}}$  is defined by:

$$\hat{\mathbf{w}}(t, \hat{\mathbf{x}}) = \frac{\partial}{\partial t} \hat{\mathcal{A}}_t(\hat{\mathbf{x}}). \quad (9)$$

For any function  $\psi(t, \cdot)$  defined on  $\Omega$ , we denote by  $\hat{\psi}(t, \cdot)$  the corresponding function defined on the reference domain  $\hat{\Omega}$  by

$$\hat{\psi}(t, \hat{\mathbf{x}}) = \psi(t, \hat{\mathcal{A}}_t(\hat{\mathbf{x}})). \quad (10)$$

For example, the velocity of the domain  $\mathbf{w}$  on the current frame is defined by

$$\mathbf{w}(t, \mathbf{x}) = \hat{\mathbf{w}}(t, \hat{\mathcal{A}}_t^{-1}(\mathbf{x})). \quad (11)$$

Notice that the functions  $\psi$  and  $\hat{\psi}$  are such that:

$$\frac{\partial \hat{\psi}}{\partial t}(t, \hat{\mathbf{x}}) = \frac{\partial \psi}{\partial t}(t, \hat{\mathcal{A}}_t(\hat{\mathbf{x}})) + \mathbf{w}(t, \hat{\mathcal{A}}_t(\hat{\mathbf{x}})) \cdot \nabla \psi(t, \hat{\mathcal{A}}_t(\hat{\mathbf{x}})). \quad (12)$$

The fact that  $\hat{\mathcal{A}}_t$  maps  $\hat{\Omega}_i$  to  $\Omega_i(t)$  ( $i = 1$  or  $2$ ) implies that the velocity of the domain satisfies

$$\mathbf{w} \cdot \mathbf{n}_i = \mathbf{u} \cdot \mathbf{n}_i \text{ on } \partial\Omega_i, \quad (13)$$

where  $i = 1$  or  $i = 2$  and  $\mathbf{n}_i$  denotes the unit outward vector normal to  $\Omega_i$ . The density  $\rho$  of the fluid is such that:

$$\rho(t, \mathbf{x}) = \hat{\rho}(\hat{\mathcal{A}}_t^{-1}(\mathbf{x})), \quad (14)$$

where  $\hat{\rho}$  is equal to  $\rho_1$  on  $\hat{\Omega}_1$  and  $\rho_2$  on  $\hat{\Omega}_2$ .

The following functional spaces will be needed, respectively for the velocity  $\mathbf{u}$  and the pressure  $p$ :

$$V = L^2(0, T; \mathbb{H}_{\mathbf{n}}^1(\Omega)), \quad M = L^2(0, T; L_0^2(\Omega)),$$

where

$$\mathbb{H}_{\mathbf{n}}^1(\Omega) = \left\{ \mathbf{u} \in (H^1(\Omega))^d, \mathbf{u} \cdot \mathbf{n}_{\partial\Omega} = 0 \text{ on } \partial\Omega \right\},$$

and

$$L_0^2(\Omega) = \left\{ p \in L^2(\Omega), \int_{\Omega} p = 0 \right\}.$$

We also introduce the test function spaces on the reference domain

$$\hat{V} = \mathbb{H}_{\mathbf{n}}^1(\hat{\Omega}), \quad \hat{M} = L_0^2(\hat{\Omega}).$$

In the moving frame, the test function spaces are defined by

$$V_T = \{ \mathbf{v} : [0, T] \times \Omega \rightarrow \mathbb{R}^d, \mathbf{v}(t, \mathbf{x}) = \hat{\mathbf{v}}(\hat{\mathcal{A}}_t^{-1}(\mathbf{x})), \hat{\mathbf{v}} \in \hat{V} \},$$

$$M_T = \{ q : [0, T] \times \Omega \rightarrow \mathbb{R}, q(t, \mathbf{x}) = \hat{q}(\hat{\mathcal{A}}_t^{-1}(\mathbf{x})), \hat{q} \in \hat{M} \}.$$

Thus, the test functions do not depend on time in the reference frame  $\hat{\Omega}$  whereas they do on the current one: more precisely, let  $\mathbf{v}$  be in  $V_T$ , then for a fixed  $\hat{\mathbf{x}} \in \hat{\Omega}$ ,  $\mathbf{v}(t, \hat{\mathcal{A}}_t(\hat{\mathbf{x}}))$  does not depend on time while for a fixed  $\mathbf{x} \in \Omega$ ,  $\mathbf{v}(t, \mathbf{x})$  does.

We are now in position to state the weak ALE formulation. It is the following coupled problem: we look for a function  $\hat{\mathcal{A}}_t : \hat{\Omega} \rightarrow \Omega$  and  $(\mathbf{u}, p)$  in  $V \times M$  such that  $\mathbf{u}(t=0, \cdot) = \mathbf{u}_0$  and:

- The function  $\hat{\mathcal{A}}_t$  is smooth and maps  $\hat{\Omega}_i$  to  $\Omega_i(t)$  ( $i = 1$  or  $2$ ). The domains  $\Omega_i(t)$  occupied by each fluid are thus defined by  $\hat{\mathcal{A}}_t$  and the density of the fluid  $\rho$  is defined by:

$$\rho(t, \mathbf{x}) = \hat{\rho}(\hat{\mathcal{A}}_t^{-1}(\mathbf{x})) = \rho_i, \quad \text{for } \mathbf{x} \in \Omega_i(t). \quad (15)$$

- For all  $(\mathbf{v}, q)$  in  $V_T \times M_T$ ,

$$\left\{ \begin{array}{l} \frac{d}{dt} \int_{\Omega} \rho \mathbf{u} \cdot \mathbf{v} + \int_{\Omega} \rho (\mathbf{u} - \mathbf{w}) \cdot \nabla \mathbf{u} \cdot \mathbf{v} - \int_{\Omega} \operatorname{div}(\mathbf{w}) \rho \mathbf{u} \cdot \mathbf{v} \\ + \int_{\Omega} \frac{\eta}{2} (\nabla \mathbf{u} + \nabla \mathbf{u}^T) : (\nabla \mathbf{v} + \nabla \mathbf{v}^T) - \int_{\Omega} p \operatorname{div}(\mathbf{v}) \\ = -\gamma \int_{\Sigma} \operatorname{tr}(\nabla_{\Sigma} \mathbf{v}) d\sigma_{\Sigma} - \beta \int_{\partial\Omega} (\mathbf{u} - \mathbf{u}^b) \cdot \mathbf{v} \\ + \gamma \int_{\partial\Sigma} \cos(\theta_s) \mathbf{t}_{\partial\Omega} \cdot \mathbf{v} dl_{\partial\Sigma} + \int_{\Omega} \mathbf{f} \cdot \mathbf{v}, \\ \int_{\Omega} q \operatorname{div}(\mathbf{u}) = 0. \end{array} \right. \quad (16)$$

### 3.2 Derivation of the weak ALE formulation

Let us explain how this weak ALE formulation is obtained from the strong formulation (1), with the boundary conditions (6)–(7). For more details, we refer to [6] or to Chapter 5 in [8]. This derivation is based on the Reynolds transport formula:

**Lemma 1** *For any smooth function  $\psi$  depending on time  $t$  and space  $\mathbf{x}$ , and any smooth function  $\phi$  such that  $\hat{\phi}$  (defined by  $\hat{\phi}(t, \hat{\mathbf{x}}) = \phi(t, \hat{\mathcal{A}}_t(\hat{\mathbf{x}}))$ ) is time-independent, we have:*

$$\begin{aligned} & \frac{d}{dt} \int_{\Omega} \psi(t, \mathbf{x}) \phi(t, \mathbf{x}) d\mathbf{x} \\ &= \int_{\Omega} \phi(t, \mathbf{x}) \frac{\partial \psi}{\partial t}(t, \mathbf{x}) + \phi(t, \mathbf{x}) \mathbf{w}(t, \mathbf{x}) \cdot \nabla \psi(t, \mathbf{x}) + \phi(t, \mathbf{x}) \operatorname{div}(\mathbf{w}(t, \mathbf{x})) \psi(t, \mathbf{x}) d\mathbf{x}. \end{aligned} \quad (17)$$

**Notation:** In Lemma 1 and in the sequel, the spatial differential operators are taken with respect to the Eulerian variable  $\mathbf{x}$ . We omit to denote this explicitly for conciseness.

The first line in (16) is obtained by multiplying the material derivative in the equation on  $\mathbf{u}$  in (1) by the test function  $\mathbf{v} \in V_T$  and integrating over  $\Omega$ :

$$\begin{aligned} \int_{\Omega} \frac{\partial(\rho \mathbf{u})}{\partial t} \cdot \mathbf{v} + \operatorname{div}(\rho \mathbf{u} \otimes \mathbf{u}) \cdot \mathbf{v} &= \int_{\Omega} \rho \frac{\partial \mathbf{u}}{\partial t} \cdot \mathbf{v} + \rho \mathbf{u} \cdot \nabla \mathbf{u} \cdot \mathbf{v}, \\ &= \frac{d}{dt} \int_{\Omega} \rho \mathbf{u} \cdot \mathbf{v} - \int_{\Omega} \rho \mathbf{w} \cdot \nabla \mathbf{u} \cdot \mathbf{v} - \operatorname{div}(\mathbf{w}) \rho \mathbf{u} \cdot \mathbf{v} + \rho \mathbf{u} \cdot \nabla \mathbf{u} \cdot \mathbf{v}, \end{aligned}$$

where we used successively the equation on  $\rho$  in (1) and then (17). The weak formulation of the terms involving the pressure are classically obtained by integration by parts. It is straightforward to obtain the following variational formulation for the term involving the viscous stress and the surface tension term:

$$\int_{\Omega} \frac{\eta}{2} (\nabla \mathbf{u} + \nabla \mathbf{u}^T) : (\nabla \mathbf{v} + \nabla \mathbf{v}^T) - \int_{\partial\Omega} \boldsymbol{\sigma} \mathbf{n}_{\partial\Omega} \cdot \mathbf{v} - \int_{\Sigma} \gamma H \mathbf{v} \cdot \mathbf{n}_{\Sigma} d\sigma_{\Sigma}. \quad (18)$$

We now use the surface divergence formula (see [20] Equation (24) p. 239 or [1], Equation (3.8)). For any smooth hypersurface  $\Sigma$  in  $\mathbb{R}^d$  (*i.e.* a submanifold of  $\mathbb{R}^d$  with codimension 1) with a smooth boundary  $\partial\Sigma$  and normal  $\mathbf{n}_{\Sigma}(\mathbf{x})$  at point  $\mathbf{x}$ , one has: for any smooth function  $\boldsymbol{\Phi} : \Sigma \rightarrow \mathbb{R}^d$ ,

$$- \int_{\Sigma} H \boldsymbol{\Phi} \cdot \mathbf{n}_{\Sigma} d\sigma_{\Sigma} = \int_{\Sigma} \operatorname{tr}(\nabla_{\Sigma} \boldsymbol{\Phi}) d\sigma_{\Sigma} - \int_{\partial\Sigma} \boldsymbol{\Phi} \cdot \mathbf{m} dl_{\partial\Sigma}, \quad (19)$$

where the surface gradient  $\nabla_{\Sigma}$  is defined by: for any smooth vector field  $\mathbf{X}$ ,

$$\nabla_{\Sigma} \mathbf{X} = P_{\Sigma}(\mathbf{x}) \nabla \mathbf{X}, \quad (20)$$

where  $P_\Sigma(\mathbf{x})$  is the orthogonal projector onto the tangent space to  $\Sigma$  at point  $\mathbf{x}$ :

$$P_\Sigma(\mathbf{x}) = \text{Id} - \mathbf{n}_\Sigma(\mathbf{x}) \otimes \mathbf{n}_\Sigma(\mathbf{x}).$$

Notice that the surface gradient of  $\mathbf{X}$  only depends on the values of  $\mathbf{X}$  on the surface  $\Sigma$ . The vector  $\mathbf{m}$  is the normal vector to  $\partial\Sigma$  in the tangent space of  $\Sigma$  pointing outwards of  $\Sigma$  (see Figure 1). The measure  $l_{\partial\Sigma}$  is the Lebesgue measure on  $\partial\Sigma$ .

Using the surface divergence formula (19), the last two terms in (18) writes:

$$\begin{aligned} - \int_{\partial\Omega} \boldsymbol{\sigma} \mathbf{n}_{\partial\Omega} \cdot \mathbf{v} - \int_\Sigma \gamma H \mathbf{v} \cdot \mathbf{n}_\Sigma d\sigma_\Sigma &= - \int_{\partial\Omega} \boldsymbol{\sigma} \mathbf{n}_{\partial\Omega} \cdot \mathbf{v} + \gamma \int_\Sigma \text{tr}(\nabla_\Sigma \mathbf{v}) d\sigma_\Sigma \\ &\quad - \gamma \int_{\partial\Sigma} \mathbf{v} \cdot \mathbf{m} dl_{\partial\Sigma}. \end{aligned} \quad (21)$$

We now use the GNBC (7) to rewrite the first and last terms in the right-hand side of (21):

$$\begin{aligned} &- \int_{\partial\Omega} \boldsymbol{\sigma} \mathbf{n}_{\partial\Omega} \cdot \mathbf{v} - \gamma \int_{\partial\Sigma} \mathbf{v} \cdot \mathbf{m} dl_{\partial\Sigma} \\ &= \beta \int_{\partial\Omega} (\mathbf{u} - \mathbf{u}^b) \cdot \mathbf{v} + \gamma \int_{\partial\Sigma} (\mathbf{m} \cdot \mathbf{t}_{\partial\Omega} - \cos(\theta_s)) \mathbf{t}_{\partial\Omega} \cdot \mathbf{v} dl_{\partial\Sigma} - \gamma \int_{\partial\Sigma} \mathbf{v} \cdot \mathbf{m} dl_{\partial\Sigma}, \\ &= \beta \int_{\partial\Omega} (\mathbf{u} - \mathbf{u}^b) \cdot \mathbf{v} - \gamma \int_{\partial\Sigma} \cos(\theta_s) \mathbf{t}_{\partial\Omega} \cdot \mathbf{v} dl_{\partial\Sigma}, \end{aligned}$$

where we have used the fact that  $\mathbf{v} \cdot \mathbf{m} = (\mathbf{v} \cdot \mathbf{t}_{\partial\Omega}) (\mathbf{m} \cdot \mathbf{t}_{\partial\Omega})$ .

With the divergence formula, we eliminate the mean curvature  $H$  (which is difficult to approximate at the discrete level), and we naturally enforce the GNBC.

### 3.3 Discretization

The discretization is based on a finite element method in space, and an implicit Euler time-discretization. The domain  $\bar{\Omega}^n = \bar{\Omega}_1^n \cup \bar{\Omega}_2^n$  at the beginning of the  $n$ -th timestep, where  $\Omega_i^n$  is the domain occupied by the fluid  $i$  at time  $t_n$ , plays the role of the reference domain  $\bar{\Omega} = \bar{\Omega}_1 \cup \bar{\Omega}_2$ .

Given the mesh  $\mathcal{M}^n = \mathcal{M}_1^n \cup \mathcal{M}_2^n$  of the domain<sup>1</sup>  $\bar{\Omega}^n = \bar{\Omega}_1^n \cup \bar{\Omega}_2^n$  and the velocity  $\mathbf{u}^n$  discretized in a finite element space at time  $t_n$ , we aim to propagate these two items to time  $t_{n+1}$ , using the weak ALE formulation (16).

In addition to  $(\mathcal{M}^n, \mathbf{u}^n)$ , let us give ourselves a space discretization of the domain velocity  $\mathbf{w}^n$  at time  $t_n$ . We will come back to its computation below, in Section 3.3.3. We introduce the application

$$\mathcal{A}_{n,n+1} : \begin{cases} (\Omega_i^n)_{i=1,2} & \rightarrow & (\Omega_i^{n+1})_{i=1,2} \\ \mathbf{y} & \mapsto & \mathbf{x} = \mathbf{y} + \delta t \mathbf{w}^n(\mathbf{y}) \end{cases}, \quad (22)$$

which might be seen as an approximation of  $\hat{\mathcal{A}}_{t_{n+1}} \circ \hat{\mathcal{A}}_{t_n}^{-1}$ . This application defines the domain occupied by each fluid<sup>2</sup> at time  $t_{n+1}$ :  $\Omega_i^{n+1} = \mathcal{A}_{n,n+1}(\Omega_i^n)$ , for  $i = 1, 2$ . Without loss of generality, the time-step  $\delta t = t_{n+1} - t_n$  is supposed to be constant. In the sequel, our convention is that  $\mathbf{y}$  denotes a point in  $(\Omega_i^n)_{i=1,2}$  and  $\mathbf{x}$  a point in  $(\Omega_i^{n+1})_{i=1,2}$ .

<sup>1</sup>and therefore the domains occupied by each fluid

<sup>2</sup> $\mathcal{A}_{n,n+1}$  also defines the mesh at time  $t_{n+1}$ : for  $i = 1, 2$ , each node of  $\mathcal{M}_i^n$  is transported from  $\Omega_i^n$  to  $\Omega_i^{n+1}$  by  $\mathcal{A}_{n,n+1}$ , thus defining the mesh  $\mathcal{M}_i^{n+1}$  of  $\Omega_i^{n+1}$  at time  $t_{n+1}$ .

### 3.3.1 Discretization in space

We consider a finite element discretization of the domain  $(\Omega_i^n)_{i=1,2}$ . It is transported by the application  $\mathcal{A}_{n,n+1}$  to a finite element discretization of the domain  $(\Omega_i^{n+1})_{i=1,2}$ . The finite element spaces at time  $t_n$  for the velocity and the pressure are respectively denoted by

$$V_{h,n} \subset \mathbb{H}_n^1(\Omega), \quad M_{h,n} \subset L_0^2(\Omega).$$

Notice that these finite element spaces depend on the time index  $n$ , since the mesh is moving. Of course, these finite element spaces need to satisfy the classical inf-sup condition. It is also possible to use the same finite element spaces for the velocity and the pressure and a stabilized variational formulation. We refer for example to [4, 10] or to Chapter 3 in [8] for more details.

As explained above, we use test functions which follow the deformation of the domain given by  $\mathcal{A}_{n,n+1}$ : the test functions at time  $t_{n+1}$  belong to the following spaces:

$$V_{h,n+1} = \{\mathbf{v}(t_{n+1}, \cdot) : \Omega \rightarrow \mathbb{R}^N, \mathbf{v}(t_{n+1}, \mathbf{x}) = \mathbf{v}(t_n, \mathcal{A}_{n,n+1}^{-1}(\mathbf{x})), \mathbf{v}(t_n, \cdot) \in V_{h,n}\},$$

$$M_{h,n+1} = \{q(t_{n+1}, \cdot) : \Omega \rightarrow \mathbb{R}, q(t_{n+1}, \mathbf{x}) = q(t_n, \mathcal{A}_{n,n+1}^{-1}(\mathbf{x})), q(t_n, \cdot) \in M_{h,n}\}.$$

Unless there is a risk of confusion, we omit the index  $h$  for the functions belonging to the finite element spaces  $V_{h,n}$  or  $M_{h,n}$ .

### 3.3.2 Time discretization and linearization

We use the following semi-implicit Euler discretization of (16): for a given  $\mathbf{u}^n \in V_{h,n}$ ,  $(\Omega_i^n)_{i=1,2}$ ,  $\mathbf{w}^n$  and  $(\Omega_i^{n+1})_{i=1,2}$ , compute  $(\mathbf{u}^{n+1}, p^{n+1}) \in V_{h,n+1} \times M_{h,n+1}$  such that, for all  $(\mathbf{v}(t_n, \cdot), q(t_n, \cdot)) \in V_{h,n} \times M_{h,n}$ ,

$$\left\{ \begin{array}{l} \frac{1}{\delta t} \int_{\Omega^{n+1}} \rho \mathbf{u}^{n+1} \cdot \mathbf{v} + \int_{\Omega^{n+1}} \rho (\mathbf{u}^n - \mathbf{w}^n) \cdot \nabla \mathbf{u}^{n+1} \cdot \mathbf{v} - \int_{\Omega^{n+1}} \operatorname{div}(\mathbf{w}^n) \rho \mathbf{u}^{n+1} \cdot \mathbf{v} \\ + \int_{\Omega^{n+1}} \frac{\eta}{2} (\nabla \mathbf{u}^{n+1} + (\nabla \mathbf{u}^{n+1})^T) : (\nabla \mathbf{v} + \nabla \mathbf{v}^T) - \int_{\Omega^{n+1}} p^{n+1} \operatorname{div}(\mathbf{v}) \\ + \int_{\Omega^{n+1}} \frac{\rho}{2} \operatorname{div}(\mathbf{u}^n) \mathbf{u}^{n+1} \cdot \mathbf{v} + \frac{\delta \rho}{2} \int_{\Sigma^{n+1}} (\mathbf{u}^n - \mathbf{w}^n) \cdot \mathbf{n}_{\Sigma^{n+1}} \mathbf{u}^{n+1} \cdot \mathbf{v} \, d\sigma_{\Sigma^{n+1}} \\ = \frac{1}{\delta t} \int_{\Omega^n} \rho \mathbf{u}^n \cdot \mathbf{v} - \gamma \int_{\Sigma^{n+1}} \operatorname{tr}(\nabla_{\Sigma^{n+1}} \mathbf{v}) \, d\sigma_{\Sigma^{n+1}} - \beta \int_{\partial \Omega^{n+1}} (\mathbf{u}^{n+1} - \mathbf{u}^b) \cdot \mathbf{v} \\ + \gamma \int_{\partial \Sigma^{n+1}} \cos(\theta_s) \mathbf{t}_{\partial \Omega} \cdot \mathbf{v} \, dl_{\partial \Sigma^{n+1}} + \int_{\Omega^{n+1}} \mathbf{f} \cdot \mathbf{v}, \\ \int_{\Omega^{n+1}} q \operatorname{div}(\mathbf{u}^{n+1}) = 0. \end{array} \right. \quad (23)$$

Notice that the superscript  $n$  (in  $\Omega^n$ ) emphasizes that we consider the domain at time  $t^n$ , even if the boundary of the domain is *not* moving. When we integrate over  $\Omega^{n+1}$ , this is to indicate that the test functions and the functions  $\rho$ ,  $\eta$  (whose values are deduced from the domains occupied by each fluid) are taken at time  $t_{n+1}$ . If a function defined on  $\Omega^n$  appears in an integral over  $\Omega^{n+1}$ , it means that this function is transported on  $\Omega^{n+1}$  by  $\mathcal{A}_{n,n+1}$ . For example,

$$\int_{\Omega^{n+1}} \frac{\rho}{2} \operatorname{div}(\mathbf{u}^n) \mathbf{u}^{n+1} \cdot \mathbf{v} = \sum_{i=1}^2 \frac{\rho_i}{2} \int_{\Omega_i^{n+1}} \operatorname{div}(\mathbf{u}^n \circ \mathcal{A}_{n,n+1}^{-1}) \mathbf{u}^{n+1} \cdot \mathbf{v}(t_{n+1}, \cdot).$$

In practice, all these integrals are easy to compute since they only involve functions which are considered at the same time ( $t_n$  or  $t_{n+1}$ ) and therefore, functions which are discretized on the same mesh.

The discretization (23) is obtained from the weak ALE formulation (16). In the third line of (23) appear two terms which are required for better stability properties of the scheme (see Section 4.2). The term  $\int_{\Omega^{n+1}} \frac{\rho}{2} \operatorname{div}(\mathbf{u}^n) \mathbf{u}^{n+1} \cdot \mathbf{v}$  is standard. It is analogous to the well-known modification introduced by Temam of the convective term (see Section III.5 in [19]) which allows to recover at the discrete level the skew-symmetry property of the advection term. The second term  $\frac{\delta\rho}{2} \int_{\Sigma^{n+1}} (\mathbf{u}^n - \mathbf{w}^n) \cdot \mathbf{n}_\Sigma \mathbf{u}^{n+1} \cdot \mathbf{v} d\sigma$  where we have used the notation

$$\delta\rho = \rho_2 - \rho_1, \quad (24)$$

is in the same vein, but is specific to the context of two-fluid flows. Notice that both these terms are strongly consistent: they vanish for the exact solution. They are introduced in order to reproduce at the discrete level the energy estimates that can be derived at the continuous level (see Section 4).

### 3.3.3 The complete algorithm

To complete the presentation of the numerical scheme, it remains to describe how the domain velocity  $\mathbf{w}^n$  is computed. The basic requirement is the kinematic condition (13), which ensures that the boundary of the domain  $\partial\Omega$  remains fixed and that the nodes of the mesh which are initially on the interface remain on the interface. In addition,  $\mathcal{A}_{n,n+1}$  defined from  $\mathbf{w}^n$  by (22) must be sufficiently smooth so that the mesh remains regular enough for finite element computations.

In the practical problems we are interested in, it seems sufficient to adopt the very standard method that consists in solving a simple Poisson problem to compute the velocity of the mesh (see [17]). Moreover, we choose the displacement to be in one direction (that we suppose, without loss of generality, to be the direction along  $\mathbf{e}_3$  in the following, where  $(\mathbf{e}_1, \mathbf{e}_2, \mathbf{e}_3)$  denotes an orthonormal basis of the physical space), so that we actually solve a *scalar* Poisson problem (see (25) below). This choice, which is definitely reasonable in the physical situations that we consider, has important favorable consequences on the quality of the algorithm. This will be made precise in Section 4.2. In addition, we discretize the velocity of the domain  $\mathbf{w}^n$  in space using the same finite element space than for the components of  $\mathbf{u}^n$ .

We may now write the complete algorithm. Let us be given  $(\Omega_i^n)_{i=1,2}$  and  $(\mathbf{u}^n, p^n)$ . Then  $\mathbf{w}^n$ ,  $(\Omega_i^{n+1})_{i=1,2}$  and  $(\mathbf{u}^{n+1}, p^{n+1})$  are computed as follows:

(i) Compute the term (defined on  $\Omega^n$ )  $\frac{1}{\delta t} \int_{\Omega^n} \rho \mathbf{u}^n \cdot \mathbf{v} d\mathbf{x}$  in the system (23).

(ii) Compute  $\mathbf{w}^n = (0, 0, w^n)$  with  $w^n$  such that

$$\begin{cases} -\Delta w^n = 0, & \text{on } \Omega_i^n, i = 1, 2, \\ w^n = \frac{\mathbf{u}^n \cdot \mathbf{n}_\Sigma}{n_\Sigma^3}, & \text{on } \Sigma^n, \\ \frac{\partial w^n}{\partial \mathbf{n}} = 0, & \text{on } \partial\Omega, \end{cases} \quad (25)$$

where the components of the normal  $\mathbf{n}_\Sigma$  are denoted  $(n_\Sigma^1, n_\Sigma^2, n_\Sigma^3)$ .

(iii) Move the nodes of the mesh according to  $\mathcal{A}_{n,n+1}$  defined by (22).

(iv) Compute the remaining terms (defined on  $\Omega^{n+1}$ ) in the system (23) (with in particular the assembling of the matrix).

- (v) Solve (23) to determine  $(\mathbf{u}^{n+1}, p^{n+1})$ . The resolution is typically performed by a GMRES iterative procedure with an ILU preconditioner and  $(\mathbf{u}^n, p^n)$  as the initial guess.

In step (ii), the implementation of the Dirichlet boundary condition on  $w$  is made easier by defining the normals  $\mathbf{n}_\Sigma$  at each node of the discretized surface  $\Sigma^n$ . Such a definition is delicate, since  $\Sigma^n$  is piecewise smooth, and the nodes are typically singular points of  $\Sigma^n$ . In practice, following [3], we use approximated normals  $\mathbf{n}_{\Sigma,h}$  at each node of the interface, by requiring that the Stokes integration by parts formula holds at the discrete level. This is one of the ingredient which ensures the exact mass conservation of each fluids on the discretized system. We refer to Section 5.1.3.2 in [8] or to [6] for more details.

## 4 Energy estimates and time-discretization

In this section, we investigate the stability of the numerical scheme in energy norm. In Section 4.1, we first derive an energy estimate at the continuous level. We then discuss in Section 4.2 to what extent the computation at the continuous level can be reproduced on the time-discretized system.

In this section, for the sake of simplicity, we suppose that the velocity of the points of the boundary of the domain is zero ( $\mathbf{u}^b = 0$ ), the static contact angle is  $\theta_s = \pi/2$  and the external force is the gravity force:  $\mathbf{f} = \rho\mathbf{g}$  where  $\mathbf{g} = -g\mathbf{e}_3$  denotes the acceleration of gravity vector.

### 4.1 An energy estimate at the continuous level

Let us first rewrite (16) in the following equivalent form:

$$\left\{ \begin{array}{l} \int_{\Omega} \frac{\partial(\rho\mathbf{u})}{\partial t} \cdot \mathbf{v} + \int_{\Omega} \operatorname{div}(\rho\mathbf{u} \otimes \mathbf{u}) \cdot \mathbf{v} + \int_{\Omega} \frac{\eta}{2} (\nabla\mathbf{u} + \nabla\mathbf{u}^T) : (\nabla\mathbf{v} + \nabla\mathbf{v}^T) - \int_{\Omega} p \operatorname{div}(\mathbf{v}) \\ = -\gamma \int_{\Sigma} \operatorname{tr}(\nabla_{\Sigma}\mathbf{v}) d\sigma_{\Sigma} - \beta \int_{\partial\Omega} \mathbf{u} \cdot \mathbf{v} + \int_{\Omega} \rho\mathbf{g} \cdot \mathbf{v}, \\ \int_{\Omega} q \operatorname{div}(\mathbf{u}) = 0. \end{array} \right. \quad (26)$$

Choosing as a test function  $\mathbf{v} = \mathbf{u}$ , we obtain:

$$\begin{aligned} & \frac{1}{2} \frac{d}{dt} \int_{\Omega} \rho |\mathbf{u}|^2 + \int_{\Omega} \frac{\eta}{2} |\nabla\mathbf{u} + \nabla\mathbf{u}^T|^2 + \beta \int_{\partial\Omega} |\mathbf{u}|^2 \\ & = -\gamma \int_{\Sigma} \operatorname{tr}(\nabla_{\Sigma}\mathbf{u}) d\sigma_{\Sigma} + \int_{\Omega} \rho\mathbf{g} \cdot \mathbf{u}. \end{aligned} \quad (27)$$

We have used the fact that:

$$\begin{aligned} \int_{\Omega} \frac{\partial(\rho\mathbf{u})}{\partial t} \cdot \mathbf{u} dx &= \int_{\Omega} \frac{\partial\rho}{\partial t} |\mathbf{u}|^2 dx + \int_{\Omega} \rho \mathbf{u} \cdot \frac{\partial\mathbf{u}}{\partial t} dx, \\ &= \int_{\Omega} \frac{\partial\rho}{\partial t} |\mathbf{u}|^2 dx + \frac{1}{2} \frac{d}{dt} \int_{\Omega} \rho |\mathbf{u}|^2 dx - \frac{1}{2} \int_{\Omega} \frac{\partial\rho}{\partial t} |\mathbf{u}|^2 dx, \\ &= \frac{1}{2} \int_{\Omega} \frac{\partial\rho}{\partial t} |\mathbf{u}|^2 dx + \frac{1}{2} \frac{d}{dt} \int_{\Omega} \rho |\mathbf{u}|^2 dx, \\ &= \frac{1}{2} \int_{\Omega} \rho \mathbf{u} \cdot \nabla(\mathbf{u}^2) dx + \frac{1}{2} \frac{d}{dt} \int_{\Omega} \rho |\mathbf{u}|^2 dx. \end{aligned}$$

Concerning the surface tension term, we have, since  $\mathbf{w} \cdot \mathbf{n}_{\partial\Omega} = 0$ ,

$$\begin{aligned} \frac{d}{dt} \int_{\Sigma} d\sigma_{\Sigma} &= \int_{\Sigma} \operatorname{tr}(\nabla_{\Sigma} \mathbf{w}) d\sigma_{\Sigma}, \\ &= \int_{\Sigma} \operatorname{tr}(\nabla_{\Sigma} \mathbf{u}) d\sigma_{\Sigma}. \end{aligned} \quad (28)$$

For the first equality, we refer for example to [2], formula (4.17) p. 355. The second equality relies on (19) and on the fact that  $\mathbf{u} \cdot \mathbf{n}_{\Sigma} = \mathbf{w} \cdot \mathbf{n}_{\Sigma}$  which implies that  $\mathbf{u} \cdot \mathbf{m} = \mathbf{w} \cdot \mathbf{m}$ .

Concerning the gravity term, we have:

$$\begin{aligned} \int_{\Omega} \rho \mathbf{g} \cdot \mathbf{u} &= - \int_{\Omega} \rho g \nabla x_3 \cdot \mathbf{u}, \\ &= \int_{\Omega} \operatorname{div}(\rho \mathbf{u}) g x_3, \\ &= - \int_{\Omega} \frac{\partial \rho}{\partial t} g x_3, \\ &= - \frac{d}{dt} \int_{\Omega} \rho g x_3, \end{aligned} \quad (29)$$

where we have used the fact that (see (24) for the definition of  $\delta\rho$ )

$$\nabla \rho = \delta\rho \mathbf{n}_{\Sigma} \delta_{\Sigma}.$$

We thus obtain the following energy estimate:

$$\frac{1}{2} \frac{d}{dt} \int_{\Omega} \rho |\mathbf{u}|^2 + \frac{d}{dt} \int_{\Omega} \rho g x_3 + \gamma \frac{d}{dt} \int_{\Sigma} d\sigma_{\Sigma} + \int_{\Omega} \frac{\eta}{2} |\nabla \mathbf{u} + \nabla \mathbf{u}^T|^2 + \beta \int_{\partial\Omega} |\mathbf{u}|^2 = 0. \quad (30)$$

## 4.2 Energy estimates at the discrete level

In this section, we present the counterparts on the time-discretized system of the computations made in last section on the continuous system. We only consider time discretization, namely the system (23) with  $(\mathbf{u}^n, p^n) \in V \times M$ . For the detailed proofs of these results, we refer to [9].

The derivation of the energy estimate at the discrete level relies on the so-called geometric conservation law (abbreviated henceforth as GCL, see [13, 5, 6]) which writes in our framework:

**Lemma 2** *Suppose that the domain velocity  $\mathbf{w}^n$  has the form  $(0, 0, w^n)$ . Let  $\phi$  be a function defined on  $\Omega_i^{n+1}$ , for  $i = 1$  or  $2$ . Then the ALE scheme satisfies the GCL in the following sense:*

$$\begin{aligned} &\int_{\Omega_i^{n+1}} \phi(\mathbf{x}) d\mathbf{x} - \int_{\Omega_i^n} \phi \circ \mathcal{A}_{n,n+1}(\mathbf{y}) d\mathbf{y} \\ &= \delta t \int_{\Omega_i^n} \phi \circ \mathcal{A}_{n,n+1}(\mathbf{y}) \operatorname{div}_{\mathbf{y}} \mathbf{w}^n(\mathbf{y}) d\mathbf{y}, \end{aligned} \quad (31)$$

$$= \delta t \int_{\Omega_i^{n+1}} \phi(\mathbf{x}) \operatorname{div}_{\mathbf{x}} \left( \mathbf{w}^n \circ \mathcal{A}_{n,n+1}^{-1}(\mathbf{x}) \right) d\mathbf{x}. \quad (32)$$

Equations (31) and (32) can be seen as discrete counterparts of the following formula: for any smooth function  $\phi$  such that  $\hat{\phi}$  (defined by  $\hat{\phi}(t, \hat{\mathbf{x}}) = \phi(t, \hat{\mathcal{A}}_t(\hat{\mathbf{x}}))$ ) is time-independent,

$$\frac{d}{dt} \int_{\Omega} \phi(t, \mathbf{x}) d\mathbf{x} = \int_{\Omega} \phi(t, \mathbf{x}) \operatorname{div} \mathbf{w}(t, \mathbf{x}) d\mathbf{x},$$

which is obtained from (17) by taking  $\psi = 1$ . The proof relies on a change of variable. We refer to [6] or to [8] for details.

Using the GCL and taking  $\mathbf{v} = \mathbf{u}^{n+1}$  as a test function in (23), one can show that:

$$\begin{aligned}
& \frac{1}{2\delta t} \left( \int_{\Omega^{n+1}} \rho |\mathbf{u}^{n+1}|^2 - \int_{\Omega^n} \rho |\mathbf{u}^n|^2 \right) + \frac{1}{\delta t} \left( \int_{\Omega^{n+2}} \rho g x_3 d\mathbf{x} - \int_{\Omega^{n+1}} \rho g x_3 d\mathbf{x} \right) + \frac{\gamma}{\delta t} (|\Sigma^{n+2}| - |\Sigma^{n+1}|) \\
& + \int_{\Omega^{n+1}} \frac{\eta}{2} |\nabla \mathbf{u}^{n+1} + (\nabla \mathbf{u}^{n+1})^T|^2 + \beta \int_{\partial\Omega} |\mathbf{u}^{n+1}|^2 \\
& = -\frac{1}{2\delta t} \int_{\Omega^n} |\mathbf{u}^{n+1} \circ \mathcal{A}_{n,n+1} - \mathbf{u}^n|^2 \\
& - \frac{\delta t}{2} \int_{\Sigma^{n+1}} \delta \rho g (w^{n+1})^2 n_{\Sigma^{n+1}}^3 + \frac{\gamma}{\delta t} \left( |\Sigma^{n+2}| - |\Sigma^{n+1}| - \delta t \int_{\Sigma^{n+1}} \text{tr}(\nabla_{\Sigma^{n+1}} \mathbf{w}^{n+1}) \right).
\end{aligned} \tag{33}$$

The estimate (33) is the discrete counterpart of (30).

The analysis of the last term in (33) (which is related to surface tension) requires the following lemma, which can be seen as a surface geometric conservation law:

**Lemma 3** *Suppose that the domain velocity  $\mathbf{w}^n$  has the form  $(0, 0, w^n)$ . Let  $\phi$  be a function defined on  $\Sigma^{n+1}$ . Then, if  $\delta t$  is sufficiently small so that*

$$1 + \delta t \text{tr}(\nabla_{\Sigma^n}(\mathbf{w}^n)) \geq 0 \quad \text{on } \Sigma_n, \tag{34}$$

the ALE scheme is such that:

$$\int_{\Sigma^{n+1}} \phi d\sigma_{\Sigma^{n+1}} - \int_{\Sigma^n} \phi \circ \mathcal{A}_{n,n+1} d\sigma_{\Sigma^n} \geq \delta t \int_{\Sigma^n} \phi \circ \mathcal{A}_{n,n+1} \text{tr}(\nabla_{\Sigma^n}(\mathbf{w}^n)) d\sigma_{\Sigma^n}. \tag{35}$$

Likewise, if  $\delta t$  is sufficiently small so that

$$1 - \delta t \text{tr}(\nabla_{\Sigma^{n+1}}(\mathbf{w}^n \circ \mathcal{A}_{n,n+1}^{-1})) \geq 0 \quad \text{on } \Sigma_{n+1}, \tag{36}$$

the ALE scheme is such that:

$$\int_{\Sigma^{n+1}} \phi d\sigma_{\Sigma^{n+1}} - \int_{\Sigma^n} \phi \circ \mathcal{A}_{n,n+1} d\sigma_{\Sigma^n} \leq \delta t \int_{\Sigma^{n+1}} \phi \text{tr}(\nabla_{\Sigma^{n+1}}(\mathbf{w}^n \circ \mathcal{A}_{n,n+1}^{-1})) d\sigma_{\Sigma^{n+1}}. \tag{37}$$

Moreover, in both cases, the difference between the two sides of the inequalities (35) and (37) is of order  $\delta t^2$  in the limit  $\delta t \rightarrow 0$ .

This can be seen as the discrete counterpart of the following formula (see (28) and [2], formula (4.17) p. 355): for any smooth function  $\phi$  such that  $\hat{\phi}$  (defined by  $\hat{\phi}(t, \hat{\mathbf{x}}) = \phi(t, \hat{\mathcal{A}}_t(\hat{\mathbf{x}}))$ ) is time independent,

$$\frac{d}{dt} \int_{\Sigma_t} \phi(t, \cdot) d\sigma_{\Sigma_t} = \int_{\Sigma_t} \phi \text{tr}(\nabla_{\Sigma_t}(\mathbf{w})) d\sigma_{\Sigma_t}.$$

For the proof of Lemma 3, we refer to [9].

Let us now comment on the energy estimate (33). First, using Lemma 3, we observe that the right-hand side is of order  $\delta t$  when  $\delta t \rightarrow 0$ . This is not a surprise since the time discretization scheme is first order.

Let us now discuss the sign of the right-hand side of (33). In the case without body forces:  $g = \gamma = 0$ , it is non positive. In this case, the time discretization scheme does not bring spurious energy in the system, which is an important property, especially when

dealing with stability questions (see [7]). Such a property is easy to obtain on a fixed mesh, but more complicated to ensure on a moving mesh. It heavily relies on the GCL.

On the other hand, if we introduce a gravity force ( $g \neq 0$ ), we see that it may introduce some energy in the system. Indeed, we observe that the second term in the right-hand side of (33) is of order  $\delta t$ , but is in general non negative: if the heavier fluid is below the lighter one (which is the case in our practical applications),  $\delta\rho \leq 0$  and  $n_{\Sigma^{n+1}}^3 \geq 0$ . Likewise, if we introduce surface tension ( $\gamma \neq 0$ ), we may bring some energy in the system. Indeed, by choosing  $\phi = 1$  in (35), we see that the last term in (33) is non negative. Moreover, we observe that in both cases (gravity and surface tension) these non negative terms are integrals over the interface between the two fluids.

These theoretical results are in agreement with our practical observations. We indeed observe that when a numerical instability occurs, it is located on the interface between the two fluids. Moreover, such instabilities are typically enhanced with increasing gravity and surface tension. In practice, we avoid such instabilities by decreasing sufficiently the timestep  $\delta t$ , and in some cases by artificially reducing the acceleration of gravity  $g$ .

The construction of a time discretization scheme of order two, or which is stable in the energy norm for the gravity and the surface tension are still open problems.

## 5 Numerical experiments

We present the results of two benchmark tests proposed in [15] involving a Couette flow for two fluids. The geometry is 2D and represented in Figure 3. The domain is periodic along  $x$ : the dashed lines, located on  $x = 0$  and  $x = 4L$  represent the periodic boundaries. The walls are defined by  $y = 0$  (bottom) and  $y = H$  (top). A velocity  $V\mathbf{e}_x$  (resp.  $-V\mathbf{e}_x$ ) is imposed on the top (resp. on the bottom) of the domain. For the first test case (the ‘‘symmetric’’ one), we took the following values of the parameters from [15] (given in reduced units):  $H = 13.6$ ,  $L = 27.2$ ,  $V = 0.25$ ,  $\rho_1 = \rho_2 = 0.81$ ,  $\eta_1 = \eta_2 = 1.95$ ,  $\gamma = 5.5$ ,  $\beta_1 = \beta_2 = 1.5$  and  $\theta_s = \pi/2$ . The parameters for the second test case (the ‘‘asymmetric’’ one) are the same except  $V = 0.20$ ,  $\beta_2 = 0.591$  and  $\theta_s$  such that  $\cos\theta_s \approx 0.38$ .

At  $t = 0$ , the interfaces separating the two fluids are straight and vertical. After a while the interfaces reach a steady state position. Let us emphasize that this behaviour is a direct result of the GNBC conditions: the interfaces would of course not converge to steady curves if we had imposed  $u_x = V$  on the top and  $u_x = -V$  on the bottom (no-slip). On the other hand, such a result cannot be obtained with pure slip boundary conditions. Figure 4 shows the velocity field at  $t = 160$  in the symmetric case. The color represents the magnitude of the velocity. The blue zone surrounding the interfaces shows that they are fixed (which means they indeed sleep with respect to the wall), whereas the remaining part of the wall is red, which corresponds to a fluid adherence on the wall. More quantitatively, Figure 5 shows the velocity on the top wall at  $t = 5$  (the contact points are still moving) and at  $t = 160$  (the contact points are fixed). Figure 6 shows the evolution in time of the velocity of a point on the contact line (which tends to zero) and of the velocity of a point on the wall far from the contact line (which tends to about 0.21, whereas a total adherence would correspond to 0.25). The stationary interfaces in the symmetric and asymmetric cases are represented on Figure 7. These results are in very good agreement with those presented in [15], which were obtained either by a continuum phase-field formulation, or by molecular dynamics simulations.

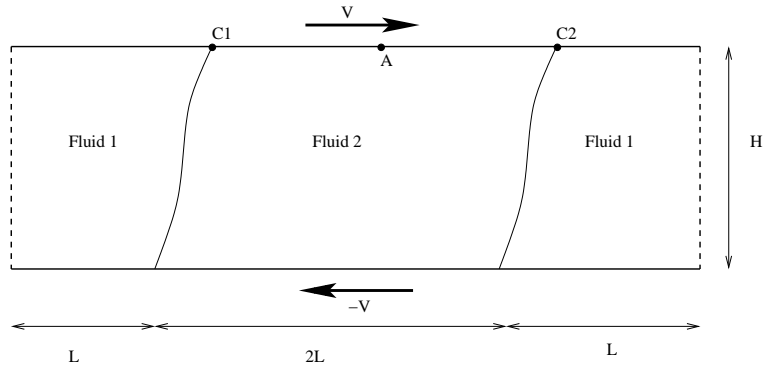


Figure 3: Schematic representation of the two-fluid periodic Couette simulation.

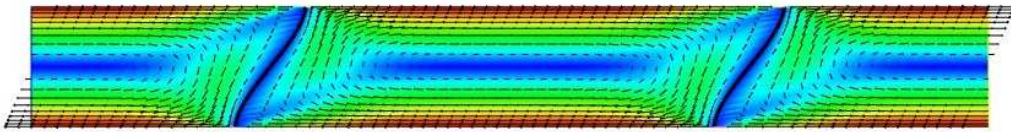


Figure 4: Velocity field at  $t=160$  (stationary state) in the symmetric case. The color represents the velocity magnitude.

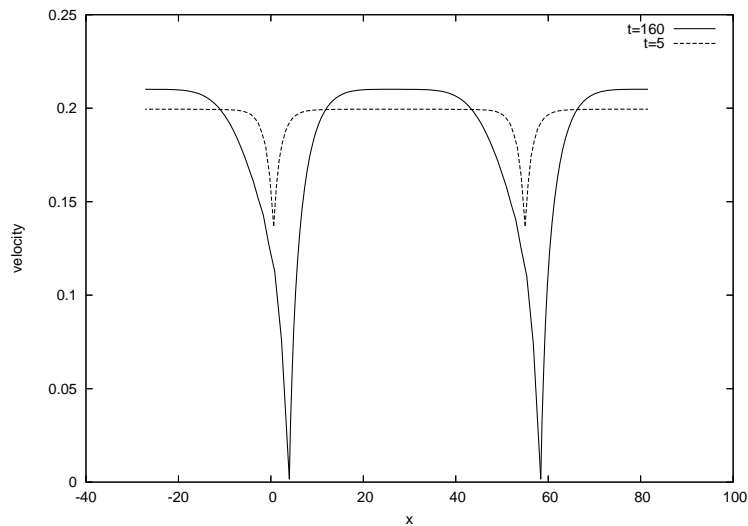


Figure 5: Velocity on the top wall *versus*  $x$  for the symmetric case. At  $t=5$ , we are still in the transient phase, the velocity of the points on the contact line is non-zero. At  $t=160$ , the points on the contact line are almost fixed (which means they indeed move with respect to the wall), whereas the points on the boundary far from the contact line move with a velocity of magnitude about 0.21 (0.25 would have meant a complete adherence on the wall).

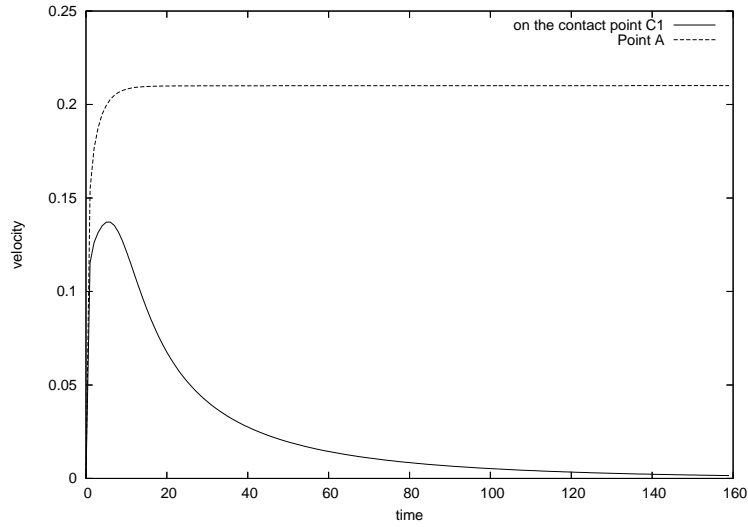


Figure 6: Velocity of the point C1 on the contact line and of the point A on the boundary (see Figure 3) *versus* time for the symmetric case. The velocity of the point on the contact line tends to zero (pure slip) whereas the velocity of the point A tends to about 0.21.

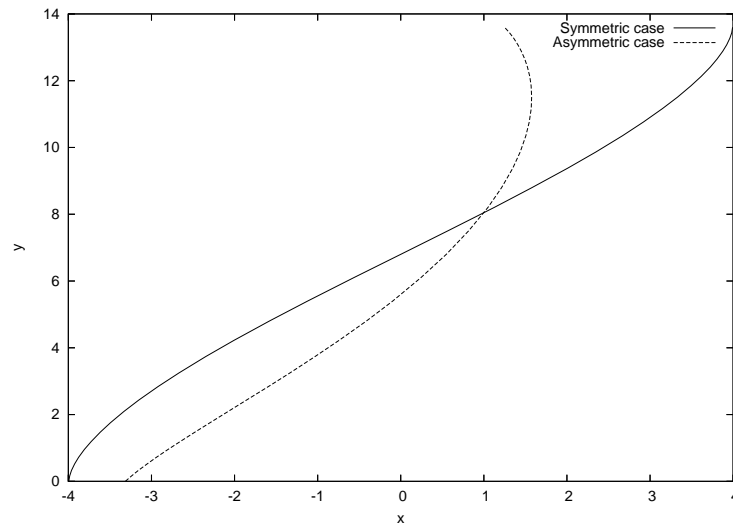


Figure 7: Interface profiles in the symmetric and asymmetric cases.

## References

- [1] L. Ambrosio and H.M. Soner. Level set approach to mean curvature flow in arbitrary codimension. *J. Differential Geom.*, 43(4):693–737, 1996.
- [2] M.C. Delfour and J.-P. Zolésio. *Shapes and Geometries*. Advances in design and control. SIAM, 2001.
- [3] M.S. Engelman, R.L. Sani, and P.M. Gresho. The implementation of normal and/or tangential velocity boundary conditions in finite element codes for incompressible fluid flow. *Int. J. Num. Meth. Fluids*, 2(3):225–238, 1982.
- [4] A. Ern and J.-L. Guermond. *Theory and practice of finite elements*. Springer Verlag, New-York, 2004.
- [5] L. Formaggia and F. Nobile. A stability analysis for the arbitrary Lagrangian Eulerian formulation with finite elements. *East-West J. Numer. Math.*, 7(2):105–131, 1999.
- [6] J.-F. Gerbeau, C. Le Bris, and T. Lelièvre. Simulations of MHD flows with moving interfaces. *Journal of Computational Physics*, 184:163–191, 2003.
- [7] J.-F. Gerbeau, C. Le Bris, and T. Lelièvre. Modelling and simulation of the industrial production of aluminium: the nonlinear approach. *Computers and Fluids*, 33:801–814, 2004.
- [8] J.-F. Gerbeau, C. Le Bris, and T. Lelièvre. *Mathematical methods for the Magneto-hydrodynamics of liquid metals*. Oxford University Press, 2006. To appear.
- [9] J.-F. Gerbeau and T. Lelièvre. *Geometric conservation law for surface tension and generalized Navier boundary condition*. In preparation.
- [10] V. Girault and P.-A. Raviart. *Finite element methods for Navier-Stokes equations*. Springer-Verlag, 1986.
- [11] D. Gueyffier, J. Li, A. Nadim, S. Scardovelli, and S. Zaleski. Volume of fluid interface tracking with smoothed surface stress methods for three-dimensional flows. *J. Comput Phys.*, 152:423–456, 1999.
- [12] C.W. Hirt and B.D. Nichols. Volume of fluids VOF method for the dynamics of free boundaries. *J. Comput. Phys.*, 39:201–225, 1981.
- [13] M. Lesoinne and C. Farhat. Geometric conservation laws for flow problems with moving boundaries and deformable meshes and their impact on aeroelastic computations. *Computer Methods in Applied Mechanics and Engineering*, 134:71–90, 1996.
- [14] T.Z. Qian, X.P. Wang, and P. Sheng. Molecular scale contact line hydrodynamics of immiscible flows. *Phys. Rev. E*, 68:016306, 2003.
- [15] T.Z. Qian, X.P. Wang, and P. Sheng. Molecular hydrodynamics of the moving contact line in two-phase immiscible flows immiscible flows. *CiCP*, 1(1):1–52, 2006.
- [16] J.A. Sethian and P. Smereka. Level set methods for fluid interfaces. *Annual Review of Fluid Mechanics*, 35:341–372, 2003.
- [17] A. Soulaïmani and Y. Saad. An arbitrary Lagrangian-Eulerian finite element method for solving three-dimensional free surface flows. *Comput. Meth Appl. Mech Engrg.*, 162:79–106, 1998.

- [18] M. Sussman, P. Smereka, and S. Osher. A level set approach for computing solutions to incompressible two-phase flow. *J. Comput. Phys.*, 114:146–159, 1994.
- [19] R. Temam. *Navier-Stokes Equations, Theory and Numerical Analysis*. North-Holland, 1979.
- [20] C.E. Weatherburn. *Differential geometry of three dimensions*, volume Volume 1. Cambridge University Press, 1947.